Microscopic and Video-Based Optical Techniques in Engineering Education

Amanda Williams, Hari Pandey, and Han Hu
Department of Mechanical Engineering, University of Arkansas, Fayetteville, AR 72701

Abstract

This paper explores the advantages of the integration of microscopic and video-based optical techniques into engineering education. Courses involving instrument training, such as Lab I, could help to provide first-year students with the ability to analyze images and videos to obtain highly precise data. This student paper explores video-based optical systems and a modular zoom lens system that were used to collect, analyze, and evaluate the nucleate boiling regime during pool boiling. Pool boiling occurs when a heated surface is submerged in a volume of liquid. The process of pool boiling provides insight into significant improvements in a surface's ability to transfer thermal energy to a fluid. Experimental analysis was completed using the OCA 15EC contact angle goniometer, a high-speed camera, and the Navitar Zoom 6000 Microscope.

Keywords

Pool Boiling, Microscope, Contact Angle Goniometer, Student Paper

Nomenclature

c	specific heat, $\frac{J}{kg*K}$
C	heat capacity rate, $\frac{W}{K}$
D	diameter, m
g	gravity, $\frac{m}{s^2}$
h	convection heat transfer coefficient, $\frac{J}{kg}$
$\overline{Nu}$	Average Nussult Number
Pr	Prandtl Number
Re	Reynolds Number
t	time, s
T	temperature, K
V	fluid velocity, $\frac{m}{s}$
$q^{"}$	heat flux, $\frac{W}{m^2}$
Greek Letters	
μ	viscosity, $\frac{kg}{s*m}$
ρ	mass density, $\frac{kg}{m^3}$
σ	surface tension, $\frac{N}{m}$
Subscripts	

b	based on a bubble
e	exit conditions
fc	forced convection
fg	based on vaporization
l	saturated liquid conditions
L	based on characteristic length
p	constant pressure conditions
s	saturated solid conditions
v	saturated vapor conditions
s	saturated solid conditions
p	constant pressure conditions
Superscripts	
m	experimentally determined value of $\frac{2}{3}$
n	constant numerical value

Introduction

Computer-based training in image-processing and video-based optical methods present a pathway to discoveries that may include the cooling of electronics, nuclear reactors, and refrigeration systems. The engineering education curriculum currently lacks the introduction to train first-year students in the technologies associated with highly effective computer-based image processing techniques. A variety of optical techniques are commonly used in engineering practices and allow the researcher to identify the fundamental mechanisms that take place in a process. In this paper, a closer look into the importance of microscopic and video-based methods in engineering is presented.

Engineering applications often require precise data acquisition that allows the engineer to develop a better understanding of the dynamics that contribute to a study. For example, superhydrophilic surfaces are of interest because they can rapidly pump or spread the liquid. Many engineers desire a surface of this nature because of its great wetting behavior. The wettability of a surface depends on surface energy and surface topology of the material. By texturing a surface with nano- or microstructures, the wetting or non-wetting behavior can be affected and bring many advantages to practical engineering applications. In this paper, the use of video-based optical techniques allows a closer look into the fundamentals of boiling, which include bubble generation, bubble growth, and bubble dynamics. The nucleate boiling regime maintains a small temperature difference which can transfer large amounts of heat between a heated surface and a fluid.

To capture the process of boiling, a high-speed camera lens was used and accompanied by an LED light source power supply. An optical table using an optical railing and three one-dimensional micrometer stages were used to allow for fine-tuning of the camera position. A modular zoom lens system provided enlarged images of the materials and was used to evaluate surface geometry. A contact angle goniometer was used to capture the dynamic wettability of the materials chosen.

Literature Review and Theory

Pool boiling occurs when a heated surface is submerged in a volume of liquid. The

process of pool boiling provides insight into significant improvements in a surface's ability to transfer thermal energy to a fluid. The motion that occurs near the surface in boiling is due to a mix of bubble growth and bubble detachment. Buoyancy forces cause the vapor bubbles to rise through the liquid and eventually escape the surface. From boiling, there is a sustained amount of heat transfer from the solid surface during the change from the liquid to the vapor state. [1] During the process of pool boiling, different boiling regimes can be understood using a boiling curve.

The pool boiling process allows a better look into the fundamental mechanisms that play a role in boiling. Free convection boiling occurs at the beginning of boiling and can be characterized by the formation of vapor bubbles. Nucleate boiling occurs after free convection and results in isolated bubbles that form at nucleation sites and then separate from the surface. This separation helps account for the increase in the convection heat transfer coefficient and the critical heat flux. It is typically desirable to operate devices in the nucleate boiling mode because of the higher heat transfer rates. When the bubble formation becomes so rapid to the point that a vapor film forms on the surface, we call this phase the transition boiling. During this state, it is expected that the boiling curve decrease. The reason why there is a decrease is that the vapor has a thermal conductivity that is lower than the liquid thermal conductivity. The effect of this is a decrease in the convection heat transfer coefficient and a decrease in critical heat flux. After transition boiling, film boiling exists in which a layer of vapor begins to cover the surface completely and in turn increases the heat flux. It is also important to note that beyond the point where the critical heat flux is reached, burnout occurs when the excess temperature exceeds the melting point of the solid.

Predicting nucleate pool boiling requires knowledge of the rate and number of surface nucleation sites during boiling. Nucleate pool boiling analysis has been shown to reflect the relationship between the surface heat flux and the excess temperature. Within the free convection boiling regime, it is typical that the action of the rising vapor bubbles may provide insight into how pool boiling data can be evaluated. The Nusselt number, a dimensionless parameter, provides a measurement of the convection heat transfer at a material's surface.

$$\overline{Nu_L} = C_{fc} Re_L^{m_{fc}} Pr^{n_{fc}} \qquad (1)$$

Since the rising vapor bubbles cause the motion of the fluid, the diameter of each bubble can be found to provide a further investigation of the pool boiling process. The diameter of a vapor bubble is determined by the buoyancy forces and the surface tension forces. Under certain conditions, vapor bubbles can rise during boiling due to gravity and the inertia of the surrounding liquid. During boiling, the spacing of the bubbles starts to decrease so much that neighboring vapor bubbles begin to collide and merge into a larger bubble. This action eventually creates a vapor layer covering the heated surface.

$$D_b \propto \sqrt{\frac{\sigma}{g(\rho_l - \rho_v)}} \qquad (2)$$

The velocity of the motion of the liquid during bubble detachment is found by dividing the vapor bubble diameter by the time it takes for the bubble to leave the surface.

$$V \propto \frac{D_b}{t_b} \propto \frac{D_b}{\left(\frac{\rho_l h_{fg} D_b^3}{q_s'' D_b^2}\right)} \propto \frac{q_s''}{\rho_l h_{fg}} \quad (3)$$

Rohsenow [2] proposed an equation that is commonly used among engineers to find the nucleate boiling heat flux. It should be noted that all properties of the liquid should be evaluated at the saturated temperature. Since the convection heat transfer coefficient decreases as the saturation pressure and saturation temperature increase. This means that the heat flux during nucleate boiling will ultimately increase as the liquid is pressurized.

$$q_s'' = \mu_l h_{fg} \left(\frac{g(\rho_l - \rho_v)}{\sigma}\right)^{1/2} \left(\frac{c_{p,l}\Delta T_e}{C_{s,f} h_{fg} Pr_l^n}\right)^3 \quad (4)$$

The average bubble size and boiling heat flux maintain a linear relationship. In this paper, this is done by converting pixels to mm^2 bubble sizes using ImageJ, and then the diameter and radius are averaged over the corresponding heat flux. It is expected that low heat fluxes will have relatively uniform bubble sizes. When the heat flux increases, the bubble size increases as well.

It also is expected that the average number of bubbles decreases exponentially due to bubble coalescence as the boiling heat flux is increased. This effect is known to be caused by the heat flux which increases the wall superheat. We will then see the bubble departure frequency increase linearly with increasing heat flux. Nanostructures will show to have a significantly enhanced bubble departure frequency. On the other hand, it should be noted that an increase in microstructures will cause a decrease in bubble departure frequency.

After bubble nucleation, the bubble diameter increases rapidly and then slows down until departure occurs. Nanostructures will show to have liquid capillary wicking effects which help to aid the formation and departure of bubbles in a rapid motion. It should be noted that nanostructures cause a decrease in bubble departure diameter. Because nanostructures can decrease bubble departure diameter and increase bubble departure frequency, it is expected that nanostructures can significantly accelerate bubble departure at low heat fluxes.

Nucleation site density is determined by the surface micro-roughness, wettability, heat flux, and wall superheat. Since it is known that nanostructures can cause accelerated bubble departure at low heat fluxes, it is expected that nanostructures will cause an increase in the number of active nucleation sites in pool boiling. In previous works, Wang and Dhir [3] have found that the active nucleation site density directly correlates to the micro-cavity radius and contact angle, but they are uncertain whether the correlation applies to nanostructures.

Video-Based Optics System Concept and Layout

A video-based optical contact angle measuring instrument, OCA 15EC, was used to collect, assess, and evaluate the measured data of static and dynamic contact angles of deionized water on various hydrophilic surfaces. The OCA 15EC contact angle goniometer uses SCA software that is designed to be used by all OCA instruments as a modular program. The SCA software enables a user to automatically measure contact hysteresis and record/store image sequences. A database of liquids and solids can be found to provide statistics and measurement error analysis for all surface energy analysis methods.

In Figure 1, an image of the contact angle goniometer setup is shown. This instrument is used for precise and reliable methods to evaluate drop contours on the plane, convex, and concave surfaces. It is important to understand contact angles when working with either hydrophobic or hydrophilic materials. By measuring the contact angle, we can find the wettability of a material. Wettability is the ability of a material to be wetted by a liquid. When a static contact angle is above 90°, the material is known to be hydrophobic and will prevent wettability. If the static contact angle is below 90°, the material is termed as hydrophilic and can be wetted. If a static contact angle is zero, or between zero and 5°, the material is considered to have maximum wettability. This means that the material has the potential to be completely wetted. A material needs to be able to be wetted during boiling. When vapor bubbles form during boiling, it is expected that a surface with higher wickability will be able to rewet the interface between the vapor bubbles and the heated surface, which enhances the critical heat flux during the boiling process.

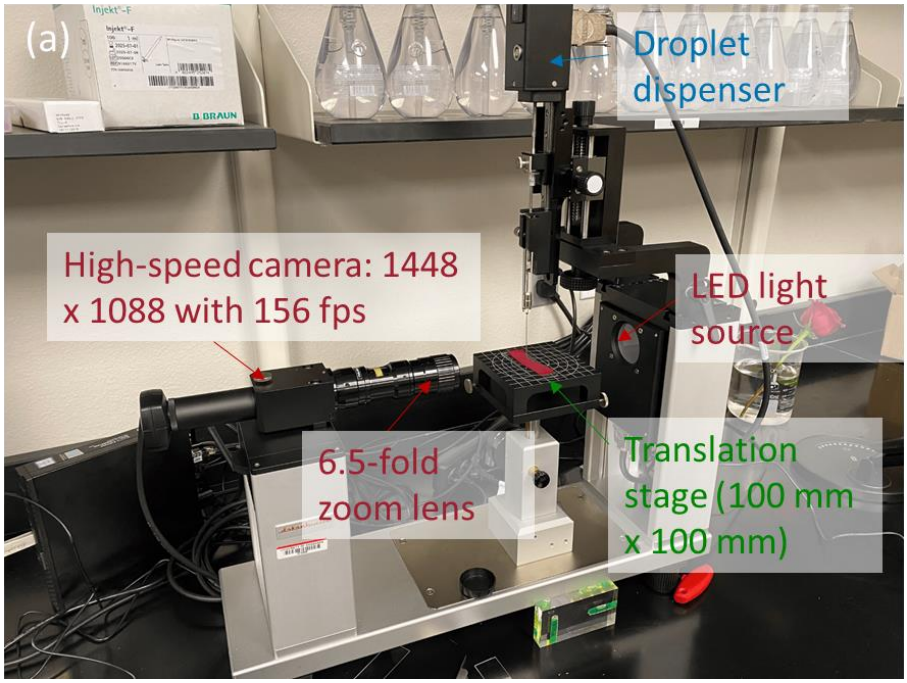

Figure 1. Experimental facility for surface wettability showing the OCA 15EC contact angle goniometer.

In Figure 2, the contact angle can indicate how the liquid will spread on a surface. A contact angle that is larger than 90 degrees is expected to have a non-wetting surface. This would indicate that the surface is quite hydrophobic. When the contact angle is less than 90 degrees, it is expected that the liquid will spread and wet the surface, indicating the surface is hydrophilic.

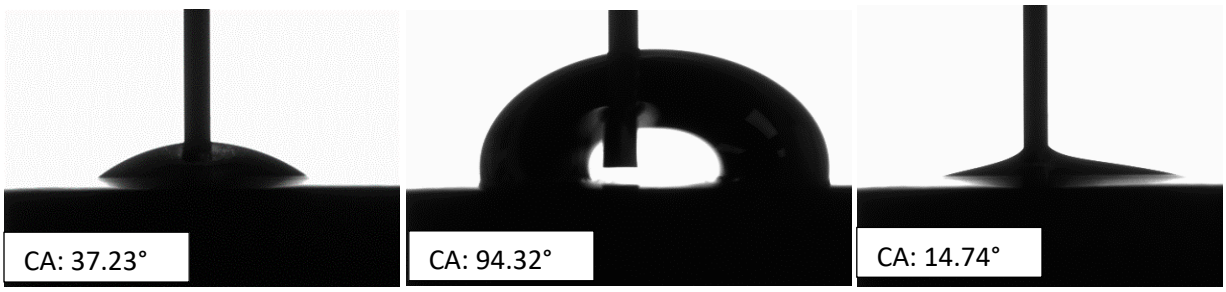

Figure 2. Profile shapes of liquid droplets on a copper block with silver nanowires where the following letters represent: (a) Static Contact Angle (b) Advancing Contact Angle (c) Receding Contact Angle

The use of the contact angle goniometer provided insight into the effects of copper oxidation. Previous studies of copper oxidation have been conducted, but the literature seems to be controversial at times. While some studies indicate that copper oxidation can cause hydrophobicity, others have found that it can also render materials to be hydrophilic. The data listed in the table below helps to provide insight into the effects of oxidation on copper.

Block A: 12-hour oxidation period	Static	Advancing	Receding
A1: Before Polishing	34.012 ± 6.73856°	85.752 ± 3.4217	15.372 ± .61555
A2: After Polishing	30.998 ± .34149	48.476 ± .31226	14.874 ± 1.2104
Block B: 24-hour oxidation period	Static	Advancing	Receding
B1: Before Polishing	40.604 ± 4.7173	94.94 ± 1.5058	14.032 ± .80566
B2: After Polishing	26.94 ± 1.3672	40.598 ± 1.8004	15.38 ± .52501

Table 1. Static and dynamic contact angle measurement results of deionized water on copper blocks with and without polishing, where A represents a copper block with silver nanoparticles with a 12-hour oxidation period and B represents a copper block with silver nanowires with a 24-hour oxidation period.

To begin experimenting on the copper block with silver nanoparticles and the copper block with silver nanowires, an oxidation period was necessary to see the effects of oxidation on copper surfaces when left out in the ambient air for different periods. The copper block with silver nanoparticles was left out to oxidize for 12 hours. In comparison, the copper block with silver nanowires was left out to oxidize for 24 hours. To begin the procedures for the experiment, a dose of 5 μL of deionized water at a rate of 2 μL/s is dispensed onto the surface. The copper block with silver nanoparticles required an ARCA (Automatic Advancing and Receding Contact Angle) dispense of 28 μL before polishing, whereas the copper block with silver nanowires required a much larger dispense of 40 μL. The settings were set to track until the user broke.

It is important to note that although B1 had a longer oxidation time, it can be determined that only a 6° difference occurred between A1 and B1. Because this is a minor difference, it is indicated that using either 12 hours or 24 hours of oxidation will result in close to similar results after polishing.

Because A1 and B1 have little difference, it can be indicated that oxidation or deposition of impurities on the surface happens rapidly.

To find evidence of the effects of oxidation on copper, the copper blocks were first prepared by polishing. The blocks were polished using wet 120 grit sandpaper, wet 320 grit sandpaper, and wet 600 grit sandpaper, followed by drying the surface with compressed air. To complete this process, one must maintain a strict polishing procedure involving the rotation of the block with each swipe on the sandpaper. It is important to do this to keep the surface smooth and free of any impurities or oxidation. The settings were set to track until the user broke. The copper block samples required an ARCA dispense of 28 μL before polishing.

The results for A2 and B2 show close to similar contact angles. When reviewing the values for the static contact angle, A2 is slightly larger when compared to B2. This difference could have been caused by more thorough polishing done with B2 than with A2. The minor difference of less than 5° indicates that A2 and B2 have the same wettability after polishing. Looking at the advancing contact angle for A2 and B2, there is at least an 8° difference that could have been due to air bubbles present in the syringe, which can cause some errors when dispensing the exact amount needed. With only about a 1° difference between the receding contact angles, it is apparent that A2 and B2 have the same wettability after polishing.

There is a slight difference when comparing the static contact angles for samples A1 and A2. It was determined that there is approximately a 4° difference while B1 and B2 resulted in a 14° difference. This difference could be caused by the oxidation or impurities present on the surface. A1 and B1 have almost twice the value for the advancing contact angle when compared to A2 and B2 respectively. Since it was noted that there was a large difference in the advancing contact angle before and after polishing, we can imply that oxidation or impurities can affect the wettability of a surface. With only a 1° difference for the receding contact angles, it is evident that oxidation or impurities deposited on the surface will not affect the boiling performance.

Microscopy

The Navitar Zoom 6000 lens system is a modular lens system that can be used to capture and analyze an enlarged image of various surfaces, as shown in Figure 3. Navitar Zoom lenses can be adjusted and keep the image in focus throughout the entire travel of the zoom range. This is called parfocal or parfocusing the system. Navitar Zoom lenses can be adjusted to line up the center of the sensor in the camera with the center of the optical zoom. This allows the lens to provide an image on the screen that does not wander laterally when the zoom is changed. This is called parcentricity or parcentering the zoom.

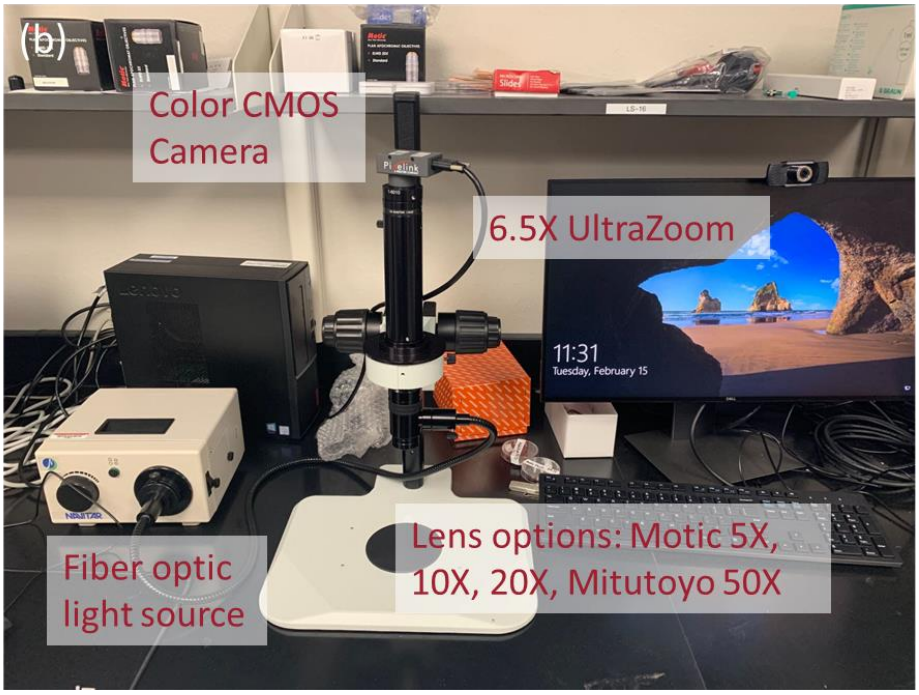

Figure 3. Experimental facility for geometry characterization showing the Navitar Zoom 6000 microscope.

With the Navitar Zoom microscope, it was found that the copper block has a structure that runs in one direction while the copper foil samples have a disorganized structure. In Figure 4, it can be seen that the copper foil with silver nanowire had a more disorganized pattern when looking at the structure. There was little difference found when comparing the sample as is and a sample with surface preparation.

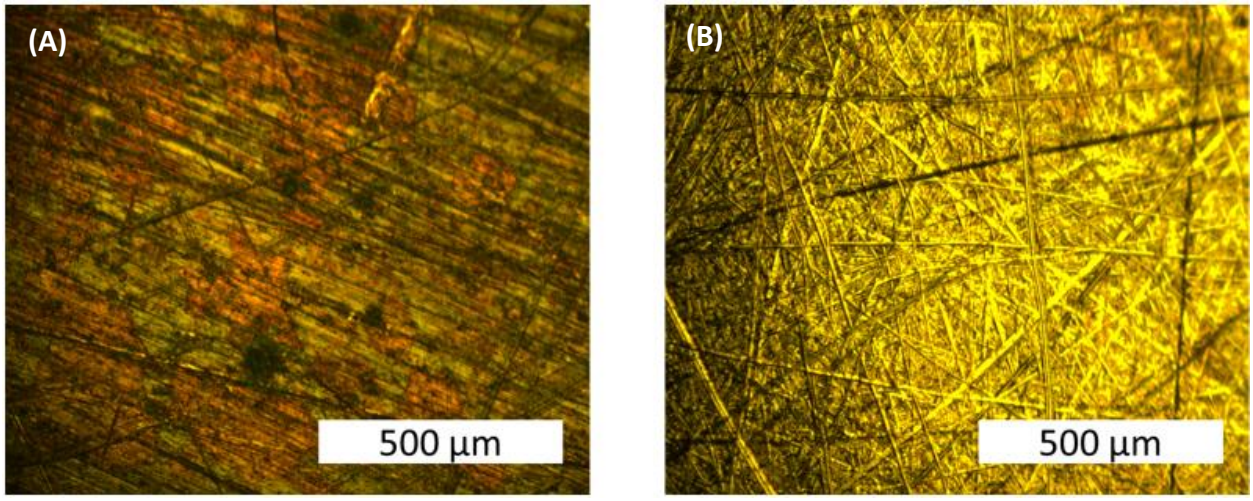

Figure 4 (A) Copper Block at 10X Magnification (B) Copper Foil with Silver Nanowires at 10X Magnification

A paper examining the hydrophilicity and surface spreading of different copper surfaces [4] concludes that copper surfaces with an increase in cavities and pores simultaneously decrease the contact angle. It is expected that smaller cavities will act as active nucleation sites on surfaces with low contact angles. Using a sanded copper surface with silver nanoparticles allows for a clear comparison between mine and Nolan's work. It was found that as the roughness of the copper surface increased, the contact angle decreased significantly. It was also found in Nolan's work that nanostructures electrodeposited on the plain copper surface provided a significant increase in the critical heat flux. Using the Navitar Zoom microscope allows the easy comparison of my work to previous works. I have found that my results clearly reflect the effects of surface roughening and nanostructured surfaces on the contact angle.

Image Processing

In this paper, temporal bubble images are captured from a high-speed camera and used for bubble analysis. The bubble size, bubble count, and several nucleation sites were analyzed to determine the bubble departure dynamics in pool boiling using hydrophilic surfaces. Data was reported based on discrete bubble departure from a single nucleation site.

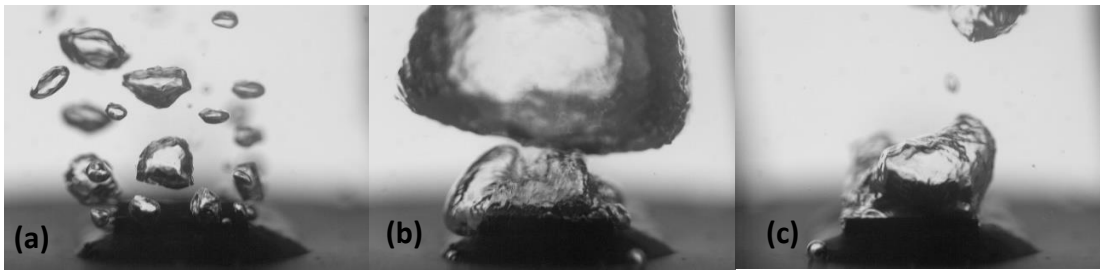

Figure 5. Images from a pool boiling experiment done on copper foam in steady-state boiling were used for bubble image analysis where the following letters represent: (a) discrete bubble departure at 15W (b) single bubble departure at 150W (c) bubble coalescence before departure at the critical heat flux.

In Figure 5, the images of measurable cases and non-measurable cases are presented. Bubbles that nucleate at different sites and coalesce before detaching from the surface create new challenges when doing bubble image analysis. When comparing single bubble boiling to coalescence boiling, boiling with coalescence results in a significant bubble and fluid motion which helps to create a large fluctuation in the surface heat flux. The bubble motion and oscillations that occur on the heater surface help to lead to frequent rewetting of the heater surface. Coalescence with nearby bubbles occurs and then the bubbles begin to depart. It's expected that with long dormant periods without bubbles on the surface, we will see sudden nucleation of multiple bubbles. As the coalescence occurs, large bubbles will begin to form and cover the heater. At this point, the departure of the large bubble will result in a sharp increase in the heat transfer rate.

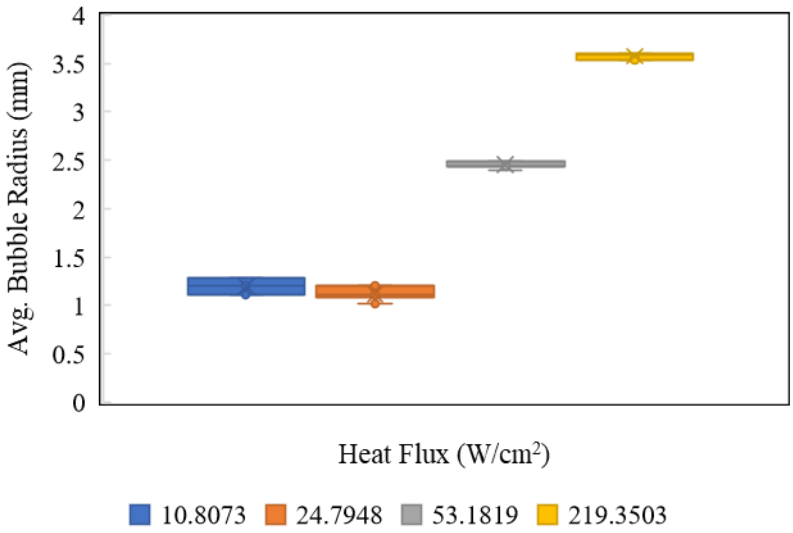

Figure 6. Average bubble diameter vs. heat flux for a boiling experiment on a copper foam surface.

The temporal bubble images captured by the high-speed camera helped to provide insight into pool boiling by using image processing techniques. To find the area of a bubble using image processing, the program ImageJ was used. Using the videos taken of the boiling process, the first 500 frames were selected to measure the area of the bubbles. Using ImageJ processing techniques, an individual discrete bubble was outlined or traced using the tracing tool. Because the bubbles tend to be larger as the heat flux increases, it was determined that using every 10 to 20 frames out of 500 frames resulted in the most accurate measurements of the bubbles. ImageJ provided the area of pixels in the traced bubble and the pixels were then converted to mm. Using the measured area, the diameter of the bubble was found. In Figure 6, the average bubble diameter was found for four separate pool boiling tests done on a copper foam surface. The graph indicates that the bubble diameter increases with increasing heat flux.

Conclusions

The engineering optical techniques mentioned in this paper help provide insight into the advantages of the integration of microscopic and video-based optical techniques into engineering education. A way to incorporate some of these practices is by training students in a lab setting on how to use the instruments properly. Integrating new optical techniques into the engineering curriculum will allow students the ability to collect, assess, and evaluate data for a variety of engineering applications.

It was found that some significant ways to produce highly precise data for analysis can be completed using video-based optics, microscopy, and image processing. The fundamental mechanisms that play a role in major engineering applications can be evaluated by all engineers if optical techniques were to be incorporated into the curriculum. Courses such as Lab I or Lab II could utilize the instruments and optical methods mentioned in this paper. Computer-based training in image-processing and video-based optical methods present a pathway to discoveries and innovative ideas.

References

[1] Theodore. L. Bergman and A. S. Lavine, *Incropera - Fundamentos de Transferência de Calor e de Massa*. 2019. [Online]. Available: https://integrada.minhabiblioteca.com.br/#/books/9788521636656/

[2] W. M. Rohsenow, P. Griffith, T. H. E. Office, and O. F. Naval, "Technical report no. 6 correlation of maximum heat flux data for boiling of saturated liquids," 1955.

[3] V. K. Dhir and S. P. Liaw, "Framework for a Unified Model for Nucleate and Transition Pool Boiling," *Journal of Heat Transfer*, vol. 111, no. 3, pp. 739–746, Aug. 1989, doi: 10.1115/1.3250745.

[4] E. Nolan, R. Rioux, P. Jiang, G. P. Peterson, and C. H. Li, "Experimental study of contact angle and active nuleation site distribution on nanostructure modified copper surface in pool boiling heat transfer enhancement," *Heat Transfer Research*, vol. 44, no. 1, pp. 115–132, 2013, doi: 10.1615/HeatTransRes.2012005687.

Amanda Williams

Amanda is an undergraduate student majoring in Mechanical Engineering at the University of Arkansas. Her research interests include engineering education and the transfer of thermal energy to a fluid. She plans to work in the industry upon graduation in May 2023.

Hari Pandey

Hari is a Ph.D. Candidate in the Department of Mechanical Engineering at the University of Arkansas. His research focus includes prediction and mitigation of boiling crisis using acoustic emission and high-speed imaging, improving boiling heat transfer using wicking structures, and immersion cooling of power electronics.

Han Hu

Han Hu is an Assistant Professor in the Department of Mechanical Engineering at the University of Arkansas. He leads the Nano Energy and Data-Driven Discovery (NED^3) Laboratory and his research interests cover experimental characterization and multi-scale modeling of two-phase heat transfer enhancement on micro-/nano-structured surfaces, immersion cooling of power electronics, diffusion kinetics in high-entropy alloys, and multimodal data fusion.